Supporting Information

Huang et al. 10.1073/pnas.1420363112

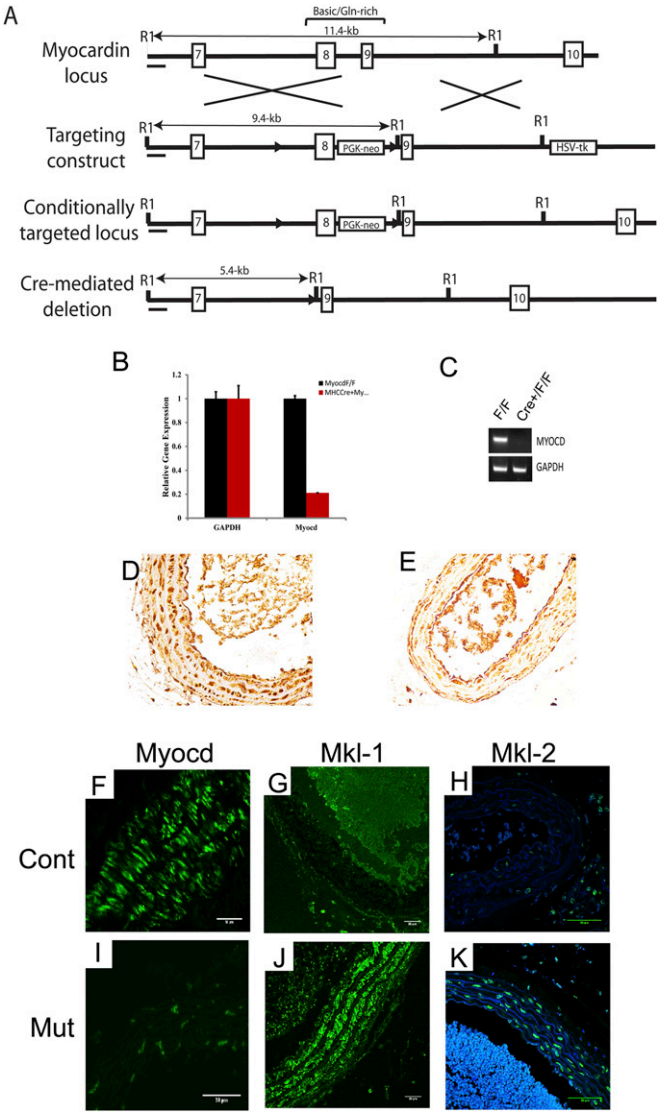

Fig. S1. Generation of mice harboring a SMC-conditional, -inducible null mutation in the *Myocd* gene. (*A*) Schematic representation of the *Myocd* gene-targeting strategy. The conditional gene-targeting construct contains the PGK–neomycin-resistance (neo) and herpes simplex virus-driven thymidine kinase (tk) genes. LoxP sites (triangles) flanking exon 8, encoding the basic and glutamine-rich domain of the myocardin protein, are shown. The conditionally targeted allele following Cre-mediated deletion is shown in the *Bottom* panel. (*B*) qRT-PCR was performed as described in *Methods* with mRNA harvested from the isolated aorta of tamoxifen-treated $Myocd^{F/F}$ control (black bars) and $SMMHC\text{-}Cre^{ERT2}/Myocd^{F/F}$ mutant (red bars) mice. The bars on left compare expression of GAPDH (control), and the bars on the right compare expression of myocardin mRNA. Data are expressed as the mean gene expression (arbitrary units) ± SEM. (*C*) Representative ethidium bromide-stained agarose gel demonstrating GAPDH (291 bp) and myocardin (108 bp) amplified gene products harvested from the aorta of control (F/F) and conditional mutant (Cre+/F/F) mice. (*D* and *E*) Immunohistochemical analysis performed with antimyocardin antibody and HRP-linked secondary antibody demonstrating markedly diminished myocardin expression (brown nuclear stain) in the SMCs populating the aorta of the tamoxifen-treated $SMMHC\text{-}Cre^{ERT2}/Myocd^{F/F}$ mutant mouse (*E*) compared with the $Myocd^{F/F}$ control (*D*). (*F–K*) Immunohistochemical analysis performed with FITC-tagged secondary antibody confirming decreased nuclear myocardin staining (green) in tamoxifen-treated $SMMHC\text{-}Cre^{ERT2}/Myocd^{F/F}$ mutant mouse (*I*) compared with the $Myocd^{F/F}$ control (*F*). By contrast, cytoplasmic Mkl-1 (*J*) and nuclear Mkl-2 (*K*) are dramatically up-regulated in the aorta of the tamoxifen-treated $SMMHC\text{-}Cre^{ERT2}/Myocd^{F/F}$ mutant mouse compared with the $Myocd^{F/F}$ control (*G* and *H*).

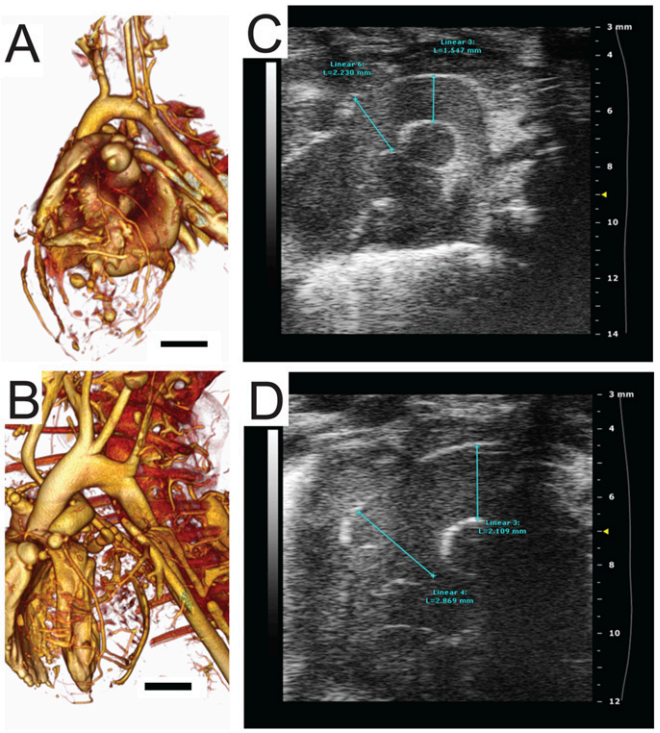

Fig. S2. Micro-CT and echocardiographic analyses of the *SMMHC-Cre^{ERT2}/Myocd$^{F/F}$* mutant aorta. (*A* and *B*) As described in *Methods*, micro-CT imaging was performed on microfil-perfused vasculature of tamoxifen-treated *Myocd$^{F/F}$* control (*A*) and *SMMHC-Cre^{ERT2}/Myocd$^{F/F}$* mutant (*B*) mice. Representative reconstructed images are displayed demonstrating dilation of the ascending aorta and aortic arch of the myocardin conditional mutant mouse (*B*) compared with the control (*A*). (Scale bar, 1 μm.) (*C* and *D*) The 2D echocardiographic analyses were performed on tamoxifen-treated *Myocd$^{F/F}$* control (*C*) and *SMMHC-Cre^{ERT2}/Myocd$^{F/F}$* mutant (*D*) mice as described in *Methods*. The diameter at the level of the aortic valve and arch of the aorta were measured (blue line) by experienced echocardiographers blinded to condition. The scale (in mm) is shown on the right of each image. Data were collected from 10 control and 10 mutant mice, 4 mo following tamoxifen treatment. Data are expressed in the *Results* section as mean aortic diameter (mm) ± SEM.

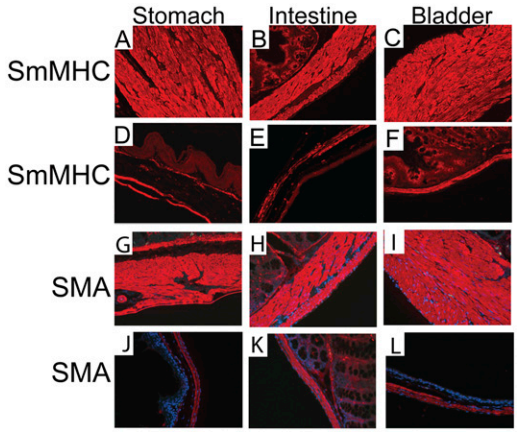

Fig. S3. Disruption and atrophy of the muscularis mucosa of gastrointestinal and urinary tracts of *Myocd* conditional mutant mice. Immunohistochemical analysis performed with SMMHC (*A*–*F*) and SMA (*G*–*L*) antibodies 4 mo after tamoxifen treatment of *Myocd$^{F/F}$* (*A*–*C* and *G*–*I*) and *SMMHC-Cre^{ERT2}/Myocd$^{F/F}$* mutant (*D*–*F* and *J*–*L*) mice. Robust SMMHC and SMA (red stain) expression is observed in visceral SMCs populating the muscularis mucosa of the stomach (*A* and *G*), small intestine (*B* and *H*), and bladder (*C* and *I*) of control mice. By contrast, relatively low level expression of SMMHC and SMA was observed in the atrophic muscularis mucosa of the stomach (*D* and *J*), small intestine (*E* and *K*), and bladder (*F* and *L*) of *SMMHC-Cre^{ERT2}/Myocd$^{F/F}$* mutant mice.

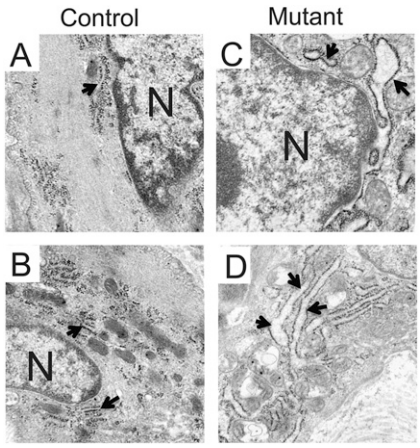

Fig. S4. Ultrastructural changes in tamoxifen-treated *SMMHC-Cre^{ERT2}/Myocd$^{F/F}$* mutant mice. At 4 mo following tamoxifen exposure, the aorta from *Myocd$^{F/F}$* (Control) and *SMMHC-Cre^{ERT2}/Myocd$^{F/F}$* mutant mice were fixed and analyzed by electron microscopy as described in *Methods*. Marked dilation of the ER (arrows), which may be indicative of ER stress/UPR, was observed in SMCs populating the aorta of *SMMHC-Cre^{ERT2}/Myocd$^{F/F}$* mutant mice (*C* and *D*) but not controls (*A* and *B*). Nuclei are denoted by "N." Original magnification, 50,000×.

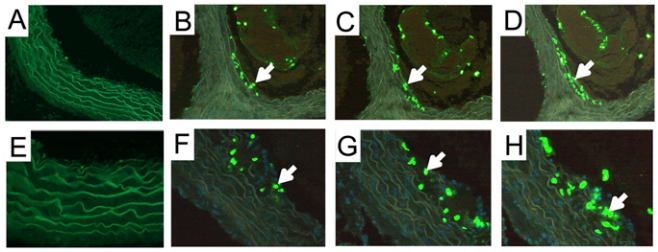

Fig. S5. Focality of TUNEL-positive medial SMCs in the aorta of *SMMHC-Cre^{ERT2}/Myocd$^{F/F}$* mutant mice. (*A–H*) Serial sections harvested from the ascending aorta were fixed and TUNEL-stained (green nuclear staining) 4 mo following tamoxifen treatment of *Myocd$^{F/F}$* control (*A* and *E*) and *SMMHC-Cre^{ERT2}/Myocd$^{F/F}$* mutant (*B–D* and *F–H*) mice. Medium- (*A*) and high- (*E*) power magnifications reveal autofluorescence of elastic lamellae with barely detectable apoptotic nuclei in the control aorta. By contrast, serial sections of the ascending aorta harvested from the *SMMHC-Cre^{ERT2}/Myocd$^{F/F}$* conditional mutant mouse (*B–D* and *F–H*) demonstrate focally distributed TUNEL-positive medial SMCs (arrows). Original magnification, 200× (*A–D*) and 400× (*E–H*).

Table S1. Antibodies used

Antibody name	Catalog no.	Company
β-tubulin	ab6046	Abcam
p62	610833	BD Transduction Laboratories
ATG5	NB110-53818	Novus
LC3	APG8B	Abgent
MLCK	EP1458Y	Novus
Fibronectin	sc-6952	Santa Cruz
Caldesmon	sc-271222	Santa Cruz
MRTF-A	sc-21558	Santa Cruz
ATG7	sc-33211	Santa Cruz
Beclin 1	NB110-87318	Novus
Myocardin	bs-9472R	Bioss
COL3A1	sc-8780-R	Santa Cruz
MKL2	HPA011286	Sigma
COL1A1	sc-25974	Santa Cruz
Collagen Type IV	AB756P	Chemicon International
Col2A1	sc-28887	Santa Cruz
Cre	C7988	Sigma
SMA	1A4	Sigma-Aldrich
SM22α	Ab10135	Abcam
Ubiquitin	AP1229a	Abgent
Phospho-eIF2a	9721L	Cell Signaling
mTOR	2983	Cell Signaling
Phospho-AMPKa	2535L	Cell Signaling
ATF-4	ab50546	Abcam
GRP78BiP	ab32618	Abcam
CHOP	sc-793	Santa Cruz Biotechnology
Sliced XBP-1	sc-7160	Santa Cruz Biotechnology
p-PERK	sc-32577	Santa Cruz Biotechnology